Raman characterization of Mg^+ ion-implanted GaN

2004 J. Phys.: Condens. Matter 16 S49

(http://iopscience.iop.org/0953-8984/16/2/006)

INSTITUTE OF PHYSICS PUBLISHING JOURNAL OF PHYSICS: CONDENSED MATTER

J. Phys.: Condens. Matter **16** (2004) S49–S55 PII: S0953-8984(04)66915-3

Raman characterization of Mg^+ ion-implanted GaN

B Boudart[1], Y Guhel[2], J C Pesant[2], P Dhamelincourt[3] and M A Poisson[4]

[1] Laboratoire Universitaire des Sciences Appliquées de Cherbourg, Site Universitaire, BP 78, 50130 Cherbourg-Octeville, France
[2] Institut d'Electronique de Microélectronique et de Nanotechnologie, UMR-CNRS 8520, Département Hyperfréquences et Semiconducteurs, Université des Sciences et Technologies de Lille, 59652 Villeneuve d'Ascq Cedex, France
[3] Laboratoire de Spectrochimie Infrarouge et Raman, UMR-CNRS 8516, Centre d'Etudes et de Recherches Lasers et Applications, Université des Sciences et Technologies de Lille, 59655 Villeneuve d'Ascq Cedex, France
[4] THALES, Laboratoire Central de Recherches, Domaine de Corbeville, 91404 Orsay Cedex, France

E-mail: bertrand.boudart@chbg.unicaen.fr

Received 31 July 2003
Published 22 December 2003
Online at stacks.iop.org/JPhysCM/16/S49 (DOI: 10.1088/0953-8984/16/2/006)

Abstract

Mg^+ ions were implanted at room temperature in n-type hexagonal GaN for the device isolation purposes. The implantation dose varied from 7.5×10^{12} to 10^{16} ions cm^{-2}. We performed resonance Raman spectroscopy and DC electrical measurements in order to monitor the structural and electrical changes of non-annealed and annealed implanted GaN samples. Annealing was carried out at 900 °C for 30 s, these conditions being used to achieve good Ohmic contacts. The aim was to determine, on the one hand, the influence of ion doses on the device isolation and, on the other, to establish the order of the technological steps which should be made between ion implantation and Ohmic contact annealing. On increasing the implantation dose from 7.5×10^{12} to 2×10^{14} ions cm^{-2}, an increase in the electrical isolation and a decrease in the photoluminescence (PL) were observed. For the highest dose, the implanted layer became conductive owing to a hopping mechanism and only the first-order phonon lines remained observable. After annealing, the implanted samples became conductive and the PL reappeared or increased compared with the non-annealed samples at same implantation doses, except for the sample implanted at the highest dose, which became insulating. Then, it is possible to achieve device electrical isolation by using a lower ion dose without thermal annealing or using a higher ion dose with thermal annealing.

1. Introduction

GaN-based devices are of interest for optical [1], high power electronic [2–4] and high temperature [5, 6] applications. During the fabrication of epitaxially based electronic devices,

the making of the device active area is realized by mesa etching using dry or wet processes or, even, by implant isolation [7]. The most important advantage of this technique is to maintain a planar wafer surface suitable for device processing. Implant isolations were achieved in GaN using H^+, He^+, N^+, F^+ and Ar^+ ions [8–12]. Moreover, the thermal stability of the implanted material is a deciding factor to consider, more particularly, during the Ohmic contact annealing operation performed at high temperature in the case of GaN [13].

Non-intentionally doped (nid) GaN is of n-type. It is possible to obtain p-type GaN by Mg doping [14] and several Raman studies were performed on this kind of material [15–17].

In this paper, we report on resonant Raman spectroscopic and electrical studies made on nid GaN samples, which were implanted with Mg^+ ions for device isolation purposes. This atomic species was chosen to compensate the electrical character of the nid material. These original studies were performed on both non-annealed and annealed samples. The aim was, on the one hand, to determine the influence of ion doses on the device isolation and, on the other, to establish the order of the technological steps which should be made between ion implantation and Ohmic contact annealing.

2. Experimental details

2.1. Sample processing

The hexagonal GaN epilayer was grown by a metal organic chemical vapour deposition process on a *c*-plane sapphire substrate. A 25 nm GaN nucleation layer followed by a 500 nm undoped GaN layer and a 200 nm n-type GaN layer with a doping level of 3×10^{17} cm^{-3} (as determined by room-temperature Hall measurements) were thus stacked. Subsequently, Ti/Al/Ni/Au (15/220/40/50 nm) metallization layers were evaporated and annealed at 900 °C for 30 s in order to achieve good Ohmic contacts, allowing us to perform the isolation's electrical measurements by the four probe method [18]. After this technological step, a sample was cut from the wafer. The short annealing time that we used at 900 °C does not damage the sample, which serves as a reference for the study [19]. The distance between the two Ohmic contacts was 5 μm and, during the implantation process, these were protected with a photoresist coating. The GaN epilayer was implanted with an Eaton 3204 implanter at room temperature with 60 keV Mg^+ ions using fluences from 7.5×10^{12} to 1×10^{16} cm^{-2}. A subsequent annealing of the implanted material was also performed at 900 °C for 30 s, under a nitrogen atmosphere, using a rapid thermal oven. All the samples were, thus, pieces cut from the same implanted wafer.

2.2. Raman spectroscopy display

Raman measurements were carried out at room temperature using 325 nm UV radiation emitted by a He–Cd laser for the excitation line with an excitation power of 1 mW on the sample surface. This particular wavelength was chosen for several reasons. Firstly, the penetration depth of the UV radiation into the material is smaller, allowing better discrimination between the Raman signal coming from the implanted zone and the one coming from the substrate underneath. Indeed, the Raman scattered light can be considered to originate from a surface layer thickness equal to $\lambda/(8\pi k) = 50$ nm, where λ and k are the laser wavelength and the cut-off coefficient at 325 nm, respectively [20]. Secondly, the GaN material is Raman resonant at this excitation wavelength, giving far better sensitivity when a very thin material layer has to be probed [21]. Thirdly, the energy of the exciting radiation is far larger than the GaN gap energy, allowing photoluminescence (PL) measurements to be made. All the measurements were performed at Jobin Yvon (Villeneuve d'Ascq, France) using a UV LABRAM Raman microspectrometer.

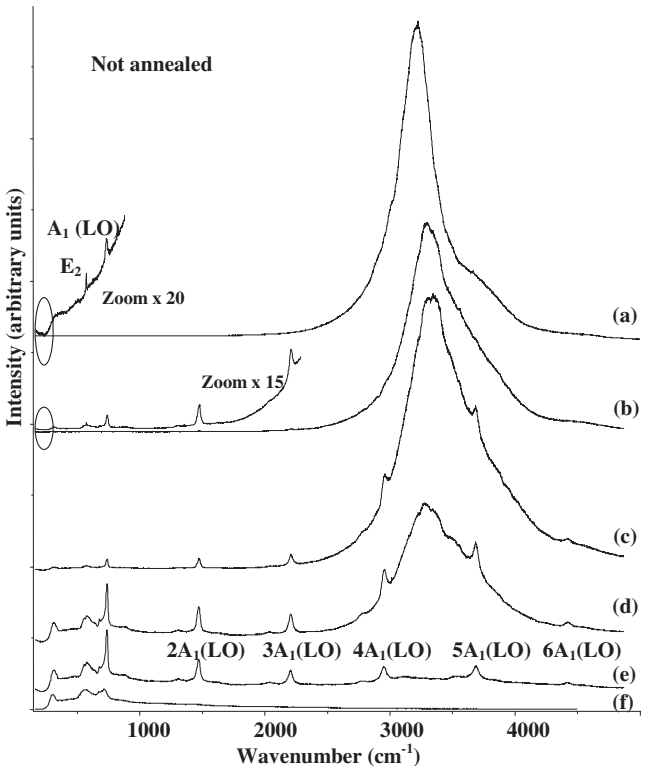

Figure 1. Raman spectra of (a) GaN as reference and samples obtained after 60 keV Mg^+ ion implantation at doses of (b) 7.5×10^{12}, (c) 1.9×10^{13}, (d) 1×10^{14}, (e) 2×10^{14} and (f) 1×10^{16} cm^{-2}.

A 100× UV objective, giving a spot size smaller than 1 μm on the sample surface, was used and the scattered light was collected using the usual $z(xy)\,\bar{z}$ microRaman backscattering geometry. In this geometry, the z direction was chosen to coincide with the hexagonal c axis. The entrance slit was opened to 100 μm, giving a 8.4 cm^{-1} spectral resolution. All the Raman lines were fitted with a Lorenzian profile in order to determine their width and position precisely.

3. Results and discussion

In figure 1, the Raman spectra of GaN before and after implantation without post annealing are shown. On the Raman spectrum of the reference sample, a strong PL structure attributed to a band to band recombination is located at 3210 cm^{-1}. Owing to this PL emission, only two Raman lines located at 569 and 728 cm^{-1} could be observed, the others being masked by the strong PL emission (see figures 1(a) and (b)). They were assigned to the E_2 and A_1 longitudinal optical (LO) modes, respectively. The observation of these Raman lines is consistent with the Raman selection rules for semiconductors having a wurtzite crystal structure [22]. On increasing the implantation dose from 7.5×10^{12} to 2×10^{14} cm^{-2}, the PL intensity strongly decreased and disappeared. The PL emission is very sensitive to the presence of extended defects and also to the presence of point defects such as impurities, vacancies and interstices which may form deep levels in the band gap, thus serving as non-radiative pathways for carrier

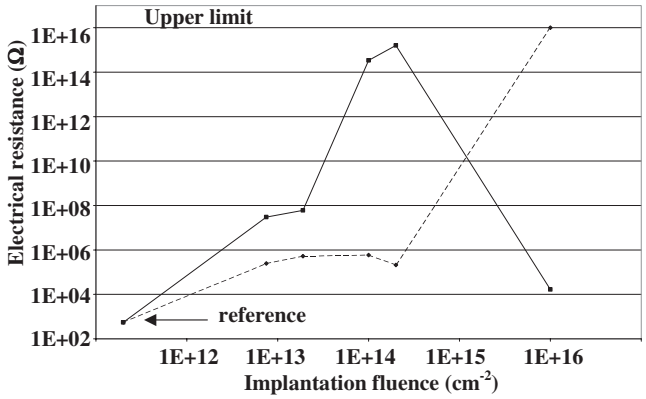

Figure 2. Evolution of the electrical resistances, versus implantation fluence, of as-implanted samples (solid line) and samples after subsequent annealing at 900 °C for 30 s (dashed line). The electrical resistance value of a non-implanted (reference) sample is shown for comparison.

recombinations [23]. At the same time, owing to the PL intensity decrease, the A_1 (LO) Raman lines become visible, and five additional Raman lines were observed at 1466, 2201, 2940, 3677, and 4412 cm^{-1} for the sample implanted with a 2×10^{14} cm^{-2} dose. These last lines were assigned to the A_1 (LO) multi-phonon scattering up to the sixth order. The observation of this high multi-phonon structure proves that the crystalline quality of the implanted samples remains fairly good. Moreover, the width at half maximum of the A_1 (LO) Raman lines slightly increases after the ion implantation (from 16 to 19 cm^{-1}, for the reference and the implanted samples with a dose of 2×10^{14} cm^{-2}, respectively). This is typically attributed to the implantation-induced damage. A Raman shift was observable for the A_1 (LO) Raman lines from 728 cm^{-1} for the reference to 733 ± 2 cm^{-1} for the implanted samples with a dose from 7.5×10^{12} to 2×10^{14} cm^{-2}. This is attributed to an implantation-induced compressive stress. Moreover, for a high 1×10^{16} cm^{-2} dose, the high order multi-phonon scattering lines disappear and the A_1 (LO) Raman line intensity strongly decreases. These observations seem very characteristic of a high dose implantation. In the Raman spectra of the more heavily damaged samples (see figures 1(c)–(e)) additional broad peaks below 700 cm^{-1} are clearly observed. This phenomenon was also observed in the same Raman configuration and in the case of GaN implanted with Ar^+, or Mg^+, or P^+, or C^+, or Ca^+ ions at high dose [12, 24]. These broad peaks could be attributed to disorder-activated Raman modes, except in our case for the band appearing at about 300 cm^{-1}, which is an artefact due to the cut-off of the dielectric filter used to suppress the exciting line. In fact, the high implantation dose that we used induces crystalline damage. Then, the wavevector conservation in the Raman scattering process breaks down and phonons from the entire Brillouin zone can be observed in the Raman spectrum. Hence the Raman spectrum reflects the total phonon density of states [25]. In the case of Ar^+ ion-implanted GaN, experiments performed by transmission electron microscopy evidenced amorphization of the implanted material [26]. This amorphous phase could also explain the disappearance of the PL emission in that case.

The electrical resistance values obtained for as-implanted samples and also for samples which were subsequently annealed at 900 °C for 30 s are presented in figure 2. These resistances were measured, at different fluences, between two Ohmic contacts separated by 5 μm. The resistance value obtained for the non-implanted GaN sample which serves as a reference is also shown for comparison. On the one hand, it was observed that, after implantation, the electrical

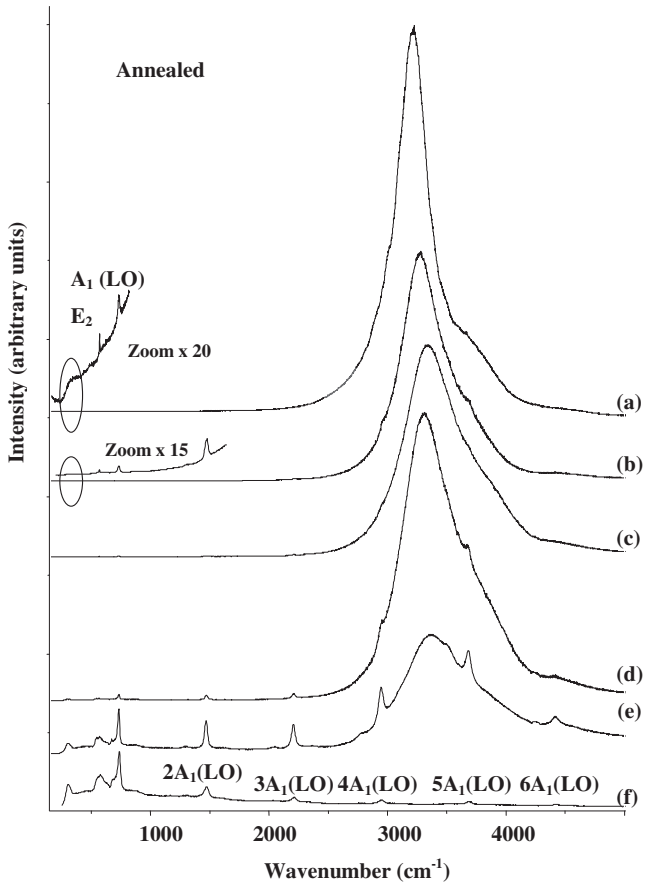

Figure 3. Raman spectra of (a) GaN as reference and samples obtained after 60 keV Mg^+ ion implantation at doses of (b) 7.5×10^{12}, (c) 1.9×10^{13}, (d) 1×10^{14}, (e) 2×10^{14} and (f) 1×10^{16} cm^{-2}, and after subsequent annealing at 900 °C for 30 s.

resistance increased as a function of the fluence and reached the very high value of 1.6×10^{15} Ω for a 2×10^{14} cm^{-2} fluence. Thus, for the highest fluence used, the sample becomes conductive, probably because of a hopping mechanism attributed to a high defect density as previously reported [27]. On the other hand, the opposite phenomenon was observed, after a subsequent annealing at 900 °C for 30 s. For a fluence up to 2×10^{14} cm^{-2}, the samples become conductive but for a higher fluence they become very resistive reaching the upper detection limit of the measurement apparatus. It is also worth noting that the electrical resistance value is always higher after implantation than before, indicating the influence of implantation.

The Raman spectra of the reference, and of the implanted GaN samples after a subsequent post-annealing at 900 °C for 30 s, are shown in figure 3. On comparison with the spectra shown in figure 1, several differences can be noted. After annealing, the PL intensity has clearly increased compared with that of non-annealed samples at the same implantation doses. This can be seen by comparing the intensity of the PL emission with that of the Raman bands. This phenomenon has also been observed in the case of Mg/P-implanted GaN after annealing performed above 1200 °C [28]. Indeed, for an implantation at a 1×10^{14} cm^{-2} fluence, the Raman lines are hardly observable because of the presence of the strong PL emission

(see figure 3(d)), whereas for a higher fluence (2×10^{14} cm^{-2}), the multi-phonon Raman and the PL structures become apparent (see figure 3(e)). Finally, for the highest fluence used, the implanted and subsequently annealed material has recovered a good crystalline quality as indicated by the observation of the A_1 (LO) multi-phonon Raman lines up to the sixth order (see figure 3(f)). After the post-implantation annealing, the width at half maximum of the A_1 (LO) phonon peak seems to decrease whatever the ion dose used. Moreover, for an ion dose from 7.5×10^{12} to 2×10^{14} cm^{-2} the A_1 (LO) phonon peak frequency decreases to 728 ± 1 cm^{-1} which is the reference value. This confirms the strong effect of the annealing for obtaining a good crystalline quality of the samples.

In the same manner as in the case of Ar^+-implanted GaN [12], it is possible to isolate electrically two different transistors by using two different approaches: first, by implanting Mg^+ ions with a 2×10^{14} cm^{-2} fluence after having performed the annealing of the Ohmic contacts and without making a further annealing, and second, by implanting Mg^+ ions with a 1×10^{16} cm^{-2} fluence followed by a subsequent annealing of the contacts in order to ensure both their Ohmic character and the recovery of their crystalline quality and also to avoid their conduction by defects which could be induced during the implantation step. The physical mechanisms involved in each case (Ar^+ or Mg^+-implanted GaN) are the same in our studies. This is probably due to the high fluences and also due to the low post-implantation annealing temperature that we used to electrically activate the species.

4. Conclusion

The influence of Mg^+ implantation fluence on the electrical isolation properties of GaN material was studied by DC electrical measurements and by resonant Raman spectroscopy. These studies allowed us to show that it is possible to achieve device electrical isolation by using a lower ion dose without thermal annealing or by using a higher ion dose with thermal annealing.

Acknowledgments

The authors gratefully acknowledge the financial support of the DGA. The Centre d'Etudes et de Recherches Lasers et Applications (CERLA) is supported by the Ministère chargé de la Recherche, the Région Nord-Pas de Calais and the Fonds Européen de Développement Economique des Régions. This work benefited from equipment made available at Jobin Yvon (Villeneuve d'Ascq, France). The authors thank M Moreau (Jobin Yvon) for her help in using the UV LABRAM instrument.

References

[1] Nakamura S, Mukai T and Senoh M 1994 *Appl. Phys. Lett.* **64** 1687
[2] Gaquière C, Trassaert S, Boudart B and Crosnier Y 2000 *IEEE Microw. Guid. Wave Lett.* **10** 19
[3] Kim H, Tilak V, Green B M, Smart J, Schaff W, Shealy J R and Eastman L K 2001 *Phys. Status Solidi* a **188** 203
[4] Eastman L K, Tilak V, Kaper V, Smart J, Thompson R, Green B M, Shealy J R and Prunty T 2002 *Phys. Status Solidi* a **194** 433
[5] Daumiller I, Kirchner C, Kamp M, Ebeling K J and Kohn E 1999 *IEEE Electron Device Lett.* **20** 448
[6] Guhel Y, Boudart B, Hoel V, Werquin M, Gaquière C, De Jaeger J C, Poisson M A, Daumiller I and Kohn E 2002 *IEE Microw. Opt. Technol. Lett.* **34** 4
[7] Williams R 1990 *Modern GaAs Processing Methods* (Boston, MA: Artech House Publishers)
[8] Binari S C, Dietrich H B, Kelner G, Rowland L B and Doverspike K 1995 *J. Appl. Phys.* **78** 3008
[9] Pearton S J, Vartuli C B, Zolper J C, Yuan C and Stall R A 1995 *Appl. Phys. Lett.* **67** 1435

[10] Wilson R G, Vartuli C B, Abernathy C R, Pearton S J and Zavada J M 1995 *Solid State Electron.* **38** 1329
[11] Zolper J C 1997 *J. Cryst. Growth* **178** 157
[12] Boudart B, Guhel Y, Pesant J C, Dhamelincourt P and Poisson M A 2002 *J. Raman Spectrosc.* **33** 283
[13] Fan Z F, Mohammad S N, Kin W, Aktas Ö, Botchkarev A E and Morkoç H 1996 *Appl. Phys. Lett.* **68** 1672
[14] Sheu J K and Chi G C 2002 *J. Phys.: Condens. Matter* **14** R657
[15] Tsen S C Y, Smith D J, Tsen K T, Kim W and Morkoç H 1997 *J. Appl. Phys.* **82** 6008
[16] Eckey L, Von Gfug U, Holst J, Hoffmann A, Kaschner A, Siegle H, Thomsen C, Schineller B, Heime K, Heuken M, Schön O and Beccard R 1998 *J. Appl. Phys.* **84** 5828
[17] Tsen K T, Koch C, Chen Y, Morkoç H, Li J, Lin J Y and Jiang H X 2000 *Appl. Phys. Lett.* **76** 2889
[18] Boudart B, Trassaert S, Wallart X, Pesant J C, Yaradou O, Théron D, Crosnier Y, Lahreche H and Omnes F 2000 *J. Electron. Mater.* **29** 603
[19] Kuball M, Demangeot F, Frandon J, Renucci M A, Massies J, Grandjean N, Aulombard R L and Briot O 1998 *Appl. Phys. Lett.* **73** 960
[20] Muth J F, Lee J H, Shmagin I K, Kolbas R M, Casey H C, Keller B P, Mishra U K and DenBaars S P 1997 *Appl. Phys. Lett.* **71** 2572
[21] Behr D, Wagner J, Schneider J, Amano H and Akasaki I 1996 *Appl. Phys. Lett.* **68** 2404
[22] Cardona M 1982 *Light Scattering in Solids II* vol 50, ed M Cardona and G Güntherodt (Berlin: Springer) p 10
[23] Popovici G, Xu G Y, Botchkarev A, Kim W, Tang H, Salvador A and Morkoç H 1997 *J. Appl. Phys.* **82** 4020
[24] Limmer W, Ritter W, Sauer R, Mensching B, Liu C and Rauschenbach B 1998 *Appl. Phys. Lett.* **72** 2589
[25] Siegle H, Kaczmarczyk G, Filippidis L, Litvinchuk A P, Hoffmann A and Thomsen C 1997 *Phys. Rev.* B **55** 7000
[26] Liu C, Mensching B, Volz K and Rauschenbach B 1997 *Appl. Phys. Lett.* **71** 2313
[27] Zolper J C, Tan H H, Williams J S, Zou J, Cockayne D J H, Pearton S J, Hagerott Crawford M and Karlicek R F 1997 *Appl. Phys. Lett.* **70** 2729
[28] Kuball M, Hayes J M, Suski T, Jun J, Leszczynski M, Domagala J, Tan H H, Williams J S and Jagadish C 2000 *J. Appl. Phys.* **87** 2736